Updated measurements of exclusive J/ψ and $\psi(2S)$ production cross-sections in pp collisions at $\sqrt{s} = 7$ TeV

LHCb Collaboration ; Bernet, R ; Müller, K ; Steinkamp, O ; Straumann, U ; Vollhardt, A ; et al

Abstract: The differential cross-section as a function of rapidity has been measured for the exclusive production of J/ψ and $\psi(2S)$ mesons in proton-proton collisions at $\sqrt{s} = 7$ TeV, using data collected by the LHCb experiment, corresponding to an integrated luminosity of 930 pb^{-1}. The cross-sections times branching fractions to two muons having pseudorapidities between 2.0 and 4.5 are measured to be

$$\begin{aligned} \sigma_{pp\to J/\psi\to\mu^+\mu^-}(2.0 < \eta_{\mu^\pm} < 4.5) = &\quad 291 \pm 7 \pm 19 \text{ pb}, \\ \sigma_{pp\to\psi(2S)\to\mu^+\mu^-}(2.0 < \eta_{\mu^\pm} < 4.5) = &\quad 6.5 \pm 0.9 \pm 0.4 \text{ pb}, \end{aligned}$$

where the first uncertainty is statistical and the second is systematic. The measurements agree with next-to-leading order QCD predictions as well as with models that include saturation effects.

DOI: https://doi.org/10.1088/0954-3899/41/5/055002

EUROPEAN ORGANIZATION FOR NUCLEAR RESEARCH (CERN)

CERN-PH-EP-2013-233
LHCb-PAPER-2013-059
24 January 2014

Updated measurements of exclusive J/ψ and $\psi(2S)$ production cross-sections in pp collisions at $\sqrt{s} = 7$ TeV

The LHCb collaboration[†]

Abstract

The differential cross-section as a function of rapidity has been measured for the exclusive production of J/ψ and $\psi(2S)$ mesons in proton-proton collisions at $\sqrt{s} = 7$ TeV, using data collected by the LHCb experiment, corresponding to an integrated luminosity of 930 pb^{-1}. The cross-sections times branching fractions to two muons having pseudorapidities between 2.0 and 4.5 are measured to be

$$\sigma_{pp\to J/\psi\to\mu^+\mu^-}(2.0 < \eta_{\mu^\pm} < 4.5) = 291 \pm 7 \pm 19\,\text{pb},$$
$$\sigma_{pp\to\psi(2S)\to\mu^+\mu^-}(2.0 < \eta_{\mu^\pm} < 4.5) = 6.5 \pm 0.9 \pm 0.4\,\text{pb},$$

where the first uncertainty is statistical and the second is systematic. The measurements agree with next-to-leading order QCD predictions as well as with models that include saturation effects.

To be submitted to Journal of Physics, G

[†]Authors are listed on the following pages.

LHCb collaboration

R. Aaij[40], B. Adeva[36], M. Adinolfi[45], A. Affolder[51], Z. Ajaltouni[5], J. Albrecht[9], F. Alessio[37], M. Alexander[50], S. Ali[40], G. Alkhazov[29], P. Alvarez Cartelle[36], A.A. Alves Jr[24], S. Amato[2], S. Amerio[21], Y. Amhis[7], L. Anderlini[17,g], J. Anderson[39], R. Andreassen[56], M. Andreotti[16,f], J.E. Andrews[57], R.B. Appleby[53], O. Aquines Gutierrez[10], F. Archilli[37], A. Artamonov[34], M. Artuso[58], E. Aslanides[6], G. Auriemma[24,n], M. Baalouch[5], S. Bachmann[11], J.J. Back[47], A. Badalov[35], V. Balagura[30], W. Baldini[16], R.J. Barlow[53], C. Barschel[38], S. Barsuk[7], W. Barter[46], V. Batozskaya[27], Th. Bauer[40], A. Bay[38], J. Beddow[50], F. Bedeschi[22], I. Bediaga[1], S. Belogurov[30], K. Belous[34], I. Belyaev[30], E. Ben-Haim[8], G. Bencivenni[18], S. Benson[49], J. Benton[45], A. Berezhnoy[31], R. Bernet[39], M.-O. Bettler[46], M. van Beuzekom[40], A. Bien[11], S. Bifani[44], T. Bird[53], A. Bizzeti[17,i], P.M. Bjørnstad[53], T. Blake[47], F. Blanc[38], J. Blouw[10], S. Blusk[58], V. Bocci[24], A. Bondar[33], N. Bondar[29], W. Bonivento[15,37], S. Borghi[53], A. Borgia[58], M. Borsato[7], T.J.V. Bowcock[51], E. Bowen[39], C. Bozzi[16], T. Brambach[9], J. van den Brand[41], J. Bressieux[38], D. Brett[53], M. Britsch[10], T. Britton[58], N.H. Brook[45], H. Brown[51], A. Bursche[39], G. Busetto[21,r], J. Buytaert[37], S. Cadeddu[15], R. Calabrese[16,f], O. Callot[7], M. Calvi[20,k], M. Calvo Gomez[35,p], A. Camboni[35], P. Campana[18,37], D. Campora Perez[37], A. Carbone[14,d], G. Carboni[23,l], R. Cardinale[19,j], A. Cardini[15], H. Carranza-Mejia[49], L. Carson[49], K. Carvalho Akiba[2], G. Casse[51], L. Castillo Garcia[37], M. Cattaneo[37], Ch. Cauet[9], R. Cenci[57], M. Charles[8], Ph. Charpentier[37], S.-F. Cheung[54], N. Chiapolini[39], M. Chrzaszcz[39,25], K. Ciba[37], X. Cid Vidal[37], G. Ciezarek[52], P.E.L. Clarke[49], M. Clemencic[37], H.V. Cliff[46], J. Closier[37], C. Coca[28], V. Coco[37], J. Cogan[6], E. Cogneras[5], P. Collins[37], A. Comerma-Montells[35], A. Contu[15,37], A. Cook[45], M. Coombes[45], S. Coquereau[8], G. Corti[37], B. Couturier[37], G.A. Cowan[49], D.C. Craik[47], M. Cruz Torres[59], S. Cunliffe[52], R. Currie[49], C. D'Ambrosio[37], J. Dalseno[45], P. David[8], P.N.Y. David[40], A. Davis[56], I. De Bonis[4], K. De Bruyn[40], S. De Capua[53], M. De Cian[11], J.M. De Miranda[1], L. De Paula[2], W. De Silva[56], P. De Simone[18], D. Decamp[4], M. Deckenhoff[9], L. Del Buono[8], N. Déléage[4], D. Derkach[54], O. Deschamps[5], F. Dettori[41], A. Di Canto[11], H. Dijkstra[37], S. Donleavy[51], F. Dordei[11], P. Dorosz[25,o], A. Dosil Suárez[36], D. Dossett[47], A. Dovbnya[42], F. Dupertuis[38], P. Durante[37], R. Dzhelyadin[34], A. Dziurda[25], A. Dzyuba[29], S. Easo[48], U. Egede[52], V. Egorychev[30], S. Eidelman[33], D. van Eijk[40], S. Eisenhardt[49], U. Eitschberger[9], R. Ekelhof[9], L. Eklund[50,37], I. El Rifai[5], Ch. Elsasser[39], A. Falabella[16,f], C. Färber[11], C. Farinelli[40], S. Farry[51], D. Ferguson[49], V. Fernandez Albor[36], F. Ferreira Rodrigues[1], M. Ferro-Luzzi[37], S. Filippov[32], M. Fiore[16,f], M. Fiorini[16,f], C. Fitzpatrick[37], M. Fontana[10], F. Fontanelli[19,j], R. Forty[37], O. Francisco[2], M. Frank[37], C. Frei[37], M. Frosini[17,37,g], E. Furfaro[23,l], A. Gallas Torreira[36], D. Galli[14,d], M. Gandelman[2], P. Gandini[58], Y. Gao[3], J. Garofoli[58], P. Garosi[53], J. Garra Tico[46], L. Garrido[35], C. Gaspar[37], R. Gauld[54], E. Gersabeck[11], M. Gersabeck[53], T. Gershon[47], Ph. Ghez[4], A. Gianelle[21], V. Gibson[46], L. Giubega[28], V.V. Gligorov[37], C. Göbel[59], D. Golubkov[30], A. Golutvin[52,30,37], A. Gomes[1,a], H. Gordon[37], M. Grabalosa Gándara[5], R. Graciani Diaz[35], L.A. Granado Cardoso[37], E. Graugés[35], G. Graziani[17], A. Grecu[28], E. Greening[54], S. Gregson[46], P. Griffith[44], L. Grillo[11], O. Grünberg[60], B. Gui[58], E. Gushchin[32], Yu. Guz[34,37], T. Gys[37], C. Hadjivasiliou[58], G. Haefeli[38], C. Haen[37], T.W. Hafkenscheid[62], S.C. Haines[46], S. Hall[52], B. Hamilton[57], T. Hampson[45], S. Hansmann-Menzemer[11], N. Harnew[54], S.T. Harnew[45], J. Harrison[53], T. Hartmann[60], J. He[37], T. Head[37], V. Heijne[40], K. Hennessy[51], P. Henrard[5], J.A. Hernando Morata[36], E. van Herwijnen[37], M. Heß[60], A. Hicheur[1], D. Hill[54], M. Hoballah[5], C. Hombach[53], W. Hulsbergen[40], P. Hunt[54], T. Huse[51], N. Hussain[54], D. Hutchcroft[51],

D. Hynds[50], V. Iakovenko[43], M. Idzik[26], P. Ilten[55], R. Jacobsson[37], A. Jaeger[11], E. Jans[40], P. Jaton[38], A. Jawahery[57], F. Jing[3], M. John[54], D. Johnson[54], C.R. Jones[46], C. Joram[37], B. Jost[37], N. Jurik[58], M. Kaballo[9], S. Kandybei[42], W. Kanso[6], M. Karacson[37], T.M. Karbach[37], I.R. Kenyon[44], T. Ketel[41], B. Khanji[20], S. Klaver[53], O. Kochebina[7], I. Komarov[38], R.F. Koopman[41], P. Koppenburg[40], M. Korolev[31], A. Kozlinskiy[40], L. Kravchuk[32], K. Kreplin[11], M. Kreps[47], G. Krocker[11], P. Krokovny[33], F. Kruse[9], M. Kucharczyk[20,25,37,k], V. Kudryavtsev[33], K. Kurek[27], T. Kvaratskheliya[30,37], V.N. La Thi[38], D. Lacarrere[37], G. Lafferty[53], A. Lai[15], D. Lambert[49], R.W. Lambert[41], E. Lanciotti[37], G. Lanfranchi[18], C. Langenbruch[37], T. Latham[47], C. Lazzeroni[44], R. Le Gac[6], J. van Leerdam[40], J.-P. Lees[4], R. Lefèvre[5], A. Leflat[31], J. Lefrançois[7], S. Leo[22], O. Leroy[6], T. Lesiak[25], B. Leverington[11], Y. Li[3], M. Liles[51], R. Lindner[37], C. Linn[11], F. Lionetto[39], B. Liu[15], G. Liu[37], S. Lohn[37], I. Longstaff[50], J.H. Lopes[2], N. Lopez-March[38], P. Lowdon[39], H. Lu[3], D. Lucchesi[21,r], J. Luisier[38], H. Luo[49], E. Luppi[16,f], O. Lupton[54], F. Machefert[7], I.V. Machikhiliyan[30], F. Maciuc[28], O. Maev[29,37], S. Malde[54], G. Manca[15,e], G. Mancinelli[6], J. Maratas[5], U. Marconi[14], P. Marino[22,t], R. Märki[38], J. Marks[11], G. Martellotti[24], A. Martens[8], A. Martín Sánchez[7], M. Martinelli[40], D. Martinez Santos[41], D. Martins Tostes[2], A. Massafferri[1], R. Matev[37], Z. Mathe[37], C. Matteuzzi[20], A. Mazurov[16,37,f], M. McCann[52], J. McCarthy[44], A. McNab[53], R. McNulty[12], B. McSkelly[51], B. Meadows[56,54], F. Meier[9], M. Meissner[11], M. Merk[40], D.A. Milanes[8], M.-N. Minard[4], J. Molina Rodriguez[59], S. Monteil[5], D. Moran[53], M. Morandin[21], P. Morawski[25], A. Mordà[6], M.J. Morello[22,t], R. Mountain[58], I. Mous[40], F. Muheim[49], K. Müller[39], R. Muresan[28], B. Muryn[26], B. Muster[38], P. Naik[45], T. Nakada[38], R. Nandakumar[48], I. Nasteva[1], M. Needham[49], S. Neubert[37], N. Neufeld[37], A.D. Nguyen[38], T.D. Nguyen[38], C. Nguyen-Mau[38,q], M. Nicol[7], V. Niess[5], R. Niet[9], N. Nikitin[31], T. Nikodem[11], A. Novoselov[34], A. Oblakowska-Mucha[26], V. Obraztsov[34], S. Oggero[40], S. Ogilvy[50], O. Okhrimenko[43], R. Oldeman[15,e], G. Onderwater[62], M. Orlandea[28], J.M. Otalora Goicochea[2], P. Owen[52], A. Oyanguren[35], B.K. Pal[58], A. Palano[13,c], M. Palutan[18], J. Panman[37], A. Papanestis[48,37], M. Pappagallo[50], L. Pappalardo[16], C. Parkes[53], C.J. Parkinson[9], G. Passaleva[17], G.D. Patel[51], M. Patel[52], C. Patrignani[19,j], C. Pavel-Nicorescu[28], A. Pazos Alvarez[36], A. Pearce[53], A. Pellegrino[40], G. Penso[24,m], M. Pepe Altarelli[37], S. Perazzini[14,d], E. Perez Trigo[36], P. Perret[5], M. Perrin-Terrin[6], L. Pescatore[44], E. Pesen[63], G. Pessina[20], K. Petridis[52], A. Petrolini[19,j], E. Picatoste Olloqui[35], B. Pietrzyk[4], T. Pilař[47], D. Pinci[24], A. Pistone[19], S. Playfer[49], M. Plo Casasus[36], F. Polci[8], G. Polok[25], A. Poluektov[47,33], E. Polycarpo[2], A. Popov[34], D. Popov[10], B. Popovici[28], C. Potterat[35], A. Powell[54], J. Prisciandaro[38], A. Pritchard[51], C. Prouve[45], V. Pugatch[43], A. Puig Navarro[38], G. Punzi[22,s], W. Qian[4], B. Rachwal[25], J.H. Rademacker[45], B. Rakotomiaramanana[38], M. Rama[18], M.S. Rangel[2], I. Raniuk[42], N. Rauschmayr[37], G. Raven[41], S. Redford[54], S. Reichert[53], M.M. Reid[47], A.C. dos Reis[1], S. Ricciardi[48], A. Richards[52], K. Rinnert[51], V. Rives Molina[35], D.A. Roa Romero[5], P. Robbe[7], D.A. Roberts[57], A.B. Rodrigues[1], E. Rodrigues[53], P. Rodriguez Perez[36], S. Roiser[37], V. Romanovsky[34], A. Romero Vidal[36], M. Rotondo[21], J. Rouvinet[38], T. Ruf[37], F. Ruffini[22], H. Ruiz[35], P. Ruiz Valls[35], G. Sabatino[24,l], J.J. Saborido Silva[36], N. Sagidova[29], P. Sail[50], B. Saitta[15,e], V. Salustino Guimaraes[2], B. Sanmartin Sedes[36], R. Santacesaria[24], C. Santamarina Rios[36], E. Santovetti[23,l], M. Sapunov[6], A. Sarti[18], C. Satriano[24,n], A. Satta[23], M. Savrie[16,f], D. Savrina[30,31], M. Schiller[41], H. Schindler[37], M. Schlupp[9], M. Schmelling[10], B. Schmidt[37], O. Schneider[38], A. Schopper[37], M.-H. Schune[7], R. Schwemmer[37], B. Sciascia[18], A. Sciubba[24], M. Seco[36], A. Semennikov[30], K. Senderowska[26], I. Sepp[52], N. Serra[39], J. Serrano[6], P. Seyfert[11], M. Shapkin[34], I. Shapoval[16,42,f], Y. Shcheglov[29], T. Shears[51], L. Shekhtman[33], O. Shevchenko[42],

V. Shevchenko[61], A. Shires[9], R. Silva Coutinho[47], G. Simi[21], M. Sirendi[46], N. Skidmore[45], T. Skwarnicki[58], N.A. Smith[51], E. Smith[54,48], E. Smith[52], J. Smith[46], M. Smith[53], M.D. Sokoloff[56], F.J.P. Soler[50], F. Soomro[38], D. Souza[45], B. Souza De Paula[2], B. Spaan[9], A. Sparkes[49], P. Spradlin[50], F. Stagni[37], S. Stahl[11], O. Steinkamp[39], S. Stevenson[54], S. Stoica[28], S. Stone[58], B. Storaci[39], S. Stracka[22,37], M. Straticiuc[28], U. Straumann[39], R. Stroili[21], V.K. Subbiah[37], L. Sun[56], W. Sutcliffe[52], S. Swientek[9], V. Syropoulos[41], M. Szczekowski[27], P. Szczypka[38,37], D. Szilard[2], T. Szumlak[26], S. T'Jampens[4], M. Teklishyn[7], G. Tellarini[16,f], E. Teodorescu[28], F. Teubert[37], C. Thomas[54], E. Thomas[37], J. van Tilburg[11], V. Tisserand[4], M. Tobin[38], S. Tolk[41], L. Tomassetti[16,f], D. Tonelli[37], S. Topp-Joergensen[54], N. Torr[54], E. Tournefier[4,52], S. Tourneur[38], M.T. Tran[38], M. Tresch[39], A. Tsaregorodtsev[6], P. Tsopelas[40], N. Tuning[40], M. Ubeda Garcia[37], A. Ukleja[27], A. Ustyuzhanin[61], U. Uwer[11], V. Vagnoni[14], G. Valenti[14], A. Vallier[7], R. Vazquez Gomez[18], P. Vazquez Regueiro[36], C. Vázquez Sierra[36], S. Vecchi[16], J.J. Velthuis[45], M. Veltri[17,h], G. Veneziano[38], M. Vesterinen[11], B. Viaud[7], D. Vieira[2], X. Vilasis-Cardona[35,p], A. Vollhardt[39], D. Volyanskyy[10], D. Voong[45], A. Vorobyev[29], V. Vorobyev[33], C. Voß[60], H. Voss[10], J.A. de Vries[40], R. Waldi[60], C. Wallace[47], R. Wallace[12], S. Wandernoth[11], J. Wang[58], D.R. Ward[46], N.K. Watson[44], A.D. Webber[53], D. Websdale[52], M. Whitehead[47], J. Wicht[37], J. Wiechczynski[25], D. Wiedner[11], L. Wiggers[40], G. Wilkinson[54], M.P. Williams[47,48], M. Williams[55], F.F. Wilson[48], J. Wimberley[57], J. Wishahi[9], W. Wislicki[27], M. Witek[25], G. Wormser[7], S.A. Wotton[46], S. Wright[46], S. Wu[3], K. Wyllie[37], Y. Xie[49,37], Z. Xing[58], Z. Yang[3], X. Yuan[3], O. Yushchenko[34], M. Zangoli[14], M. Zavertyaev[10,b], F. Zhang[3], L. Zhang[58], W.C. Zhang[12], Y. Zhang[3], A. Zhelezov[11], A. Zhokhov[30], L. Zhong[3], A. Zvyagin[37].

[1] *Centro Brasileiro de Pesquisas Físicas (CBPF), Rio de Janeiro, Brazil*
[2] *Universidade Federal do Rio de Janeiro (UFRJ), Rio de Janeiro, Brazil*
[3] *Center for High Energy Physics, Tsinghua University, Beijing, China*
[4] *LAPP, Université de Savoie, CNRS/IN2P3, Annecy-Le-Vieux, France*
[5] *Clermont Université, Université Blaise Pascal, CNRS/IN2P3, LPC, Clermont-Ferrand, France*
[6] *CPPM, Aix-Marseille Université, CNRS/IN2P3, Marseille, France*
[7] *LAL, Université Paris-Sud, CNRS/IN2P3, Orsay, France*
[8] *LPNHE, Université Pierre et Marie Curie, Université Paris Diderot, CNRS/IN2P3, Paris, France*
[9] *Fakultät Physik, Technische Universität Dortmund, Dortmund, Germany*
[10] *Max-Planck-Institut für Kernphysik (MPIK), Heidelberg, Germany*
[11] *Physikalisches Institut, Ruprecht-Karls-Universität Heidelberg, Heidelberg, Germany*
[12] *School of Physics, University College Dublin, Dublin, Ireland*
[13] *Sezione INFN di Bari, Bari, Italy*
[14] *Sezione INFN di Bologna, Bologna, Italy*
[15] *Sezione INFN di Cagliari, Cagliari, Italy*
[16] *Sezione INFN di Ferrara, Ferrara, Italy*
[17] *Sezione INFN di Firenze, Firenze, Italy*
[18] *Laboratori Nazionali dell'INFN di Frascati, Frascati, Italy*
[19] *Sezione INFN di Genova, Genova, Italy*
[20] *Sezione INFN di Milano Bicocca, Milano, Italy*
[21] *Sezione INFN di Padova, Padova, Italy*
[22] *Sezione INFN di Pisa, Pisa, Italy*
[23] *Sezione INFN di Roma Tor Vergata, Roma, Italy*
[24] *Sezione INFN di Roma La Sapienza, Roma, Italy*
[25] *Henryk Niewodniczanski Institute of Nuclear Physics Polish Academy of Sciences, Kraków, Poland*
[26] *AGH - University of Science and Technology, Faculty of Physics and Applied Computer Science, Kraków, Poland*

[27] National Center for Nuclear Research (NCBJ), Warsaw, Poland
[28] Horia Hulubei National Institute of Physics and Nuclear Engineering, Bucharest-Magurele, Romania
[29] Petersburg Nuclear Physics Institute (PNPI), Gatchina, Russia
[30] Institute of Theoretical and Experimental Physics (ITEP), Moscow, Russia
[31] Institute of Nuclear Physics, Moscow State University (SINP MSU), Moscow, Russia
[32] Institute for Nuclear Research of the Russian Academy of Sciences (INR RAN), Moscow, Russia
[33] Budker Institute of Nuclear Physics (SB RAS) and Novosibirsk State University, Novosibirsk, Russia
[34] Institute for High Energy Physics (IHEP), Protvino, Russia
[35] Universitat de Barcelona, Barcelona, Spain
[36] Universidad de Santiago de Compostela, Santiago de Compostela, Spain
[37] European Organization for Nuclear Research (CERN), Geneva, Switzerland
[38] Ecole Polytechnique Fédérale de Lausanne (EPFL), Lausanne, Switzerland
[39] Physik-Institut, Universität Zürich, Zürich, Switzerland
[40] Nikhef National Institute for Subatomic Physics, Amsterdam, The Netherlands
[41] Nikhef National Institute for Subatomic Physics and VU University Amsterdam, Amsterdam, The Netherlands
[42] NSC Kharkiv Institute of Physics and Technology (NSC KIPT), Kharkiv, Ukraine
[43] Institute for Nuclear Research of the National Academy of Sciences (KINR), Kyiv, Ukraine
[44] University of Birmingham, Birmingham, United Kingdom
[45] H.H. Wills Physics Laboratory, University of Bristol, Bristol, United Kingdom
[46] Cavendish Laboratory, University of Cambridge, Cambridge, United Kingdom
[47] Department of Physics, University of Warwick, Coventry, United Kingdom
[48] STFC Rutherford Appleton Laboratory, Didcot, United Kingdom
[49] School of Physics and Astronomy, University of Edinburgh, Edinburgh, United Kingdom
[50] School of Physics and Astronomy, University of Glasgow, Glasgow, United Kingdom
[51] Oliver Lodge Laboratory, University of Liverpool, Liverpool, United Kingdom
[52] Imperial College London, London, United Kingdom
[53] School of Physics and Astronomy, University of Manchester, Manchester, United Kingdom
[54] Department of Physics, University of Oxford, Oxford, United Kingdom
[55] Massachusetts Institute of Technology, Cambridge, MA, United States
[56] University of Cincinnati, Cincinnati, OH, United States
[57] University of Maryland, College Park, MD, United States
[58] Syracuse University, Syracuse, NY, United States
[59] Pontifícia Universidade Católica do Rio de Janeiro (PUC-Rio), Rio de Janeiro, Brazil, associated to [2]
[60] Institut für Physik, Universität Rostock, Rostock, Germany, associated to [11]
[61] National Research Centre Kurchatov Institute, Moscow, Russia, associated to [30]
[62] KVI - University of Groningen, Groningen, The Netherlands, associated to [40]
[63] Celal Bayar University, Manisa, Turkey, associated to [37]

[a] Universidade Federal do Triângulo Mineiro (UFTM), Uberaba-MG, Brazil
[b] P.N. Lebedev Physical Institute, Russian Academy of Science (LPI RAS), Moscow, Russia
[c] Università di Bari, Bari, Italy
[d] Università di Bologna, Bologna, Italy
[e] Università di Cagliari, Cagliari, Italy
[f] Università di Ferrara, Ferrara, Italy
[g] Università di Firenze, Firenze, Italy
[h] Università di Urbino, Urbino, Italy
[i] Università di Modena e Reggio Emilia, Modena, Italy
[j] Università di Genova, Genova, Italy
[k] Università di Milano Bicocca, Milano, Italy
[l] Università di Roma Tor Vergata, Roma, Italy
[m] Università di Roma La Sapienza, Roma, Italy

[n] *Università della Basilicata, Potenza, Italy*
[o] *AGH - University of Science and Technology, Faculty of Computer Science, Electronics and Telecommunications, Kraków, Poland*
[p] *LIFAELS, La Salle, Universitat Ramon Llull, Barcelona, Spain*
[q] *Hanoi University of Science, Hanoi, Viet Nam*
[r] *Università di Padova, Padova, Italy*
[s] *Università di Pisa, Pisa, Italy*
[t] *Scuola Normale Superiore, Pisa, Italy*

1 Introduction

Exclusive J/ψ and $\psi(2S)$ meson production in hadron collisions are diffractive processes that can be calculated in perturbative quantum chromodynamics (QCD) [1]. At leading order they are thought to proceed via the exchange of a photon and a pomeron, which at sufficiently hard scales can be described by two gluons as shown in Fig. 1(a). Measurements of exclusive J/ψ and $\psi(2S)$ production thus provide a test of QCD and shed light on the pomeron, which plays a critical role in the description of diffraction and soft processes. In particular, the measurements are sensitive to saturation effects [2,3]: when performed in the pseudorapidity range of the LHCb detector they probe x, the fractional momentum of the parton, down to 5×10^{-6}. Since the theoretical predictions depend on the gluon parton density function (PDF), the experimental measurements can be used to constrain it [4,5]. Furthermore, the measurements are sensitive to the presence of the odderon [6], the odd-parity partner of the pomeron, which could mediate the reaction in place of the photon in Fig. 1(a).

Several measurements of exclusive J/ψ production have been reported by the H1 [7,8] and ZEUS [9] collaborations at the HERA ep collider, at values of W, the centre-of-mass energy of the photon-proton system, between 30 and 300 GeV. The first measurement at a hadron machine, at $W \approx 80\,\text{GeV}$, was made by the CDF collaboration [10] at the Tevatron $p\bar{p}$ collider. The first measurement in pp collisions was made by the LHCb collaboration [11] using data corresponding to an integrated luminosity of $37\,\text{pb}^{-1}$ collected at $\sqrt{s} = 7\,\text{TeV}$, and this extended the W reach up to 1.5 TeV. Measurements in Pb-Pb collisions at the LHC have been reported by the ALICE collaboration [12]. Measurements of $\psi(2S)$ production have been made by the H1 collaboration [13] at four W values while both CDF [10] and LHCb [11] reported results using small samples of $\psi(2S)$ consisting of about 40 candidates each.

The J/ψ photoproduction cross-section has been fit by a power-law function, $\sigma_{\gamma p \to J/\psi p}(W) = a(W/90\,\text{GeV})^{\delta}$, with the H1 collaboration measuring $a = 81 \pm 3\,\text{pb}$ and $\delta = 0.67 \pm 0.03$ [8]. At leading order this follows from the small-x parametrisation of the

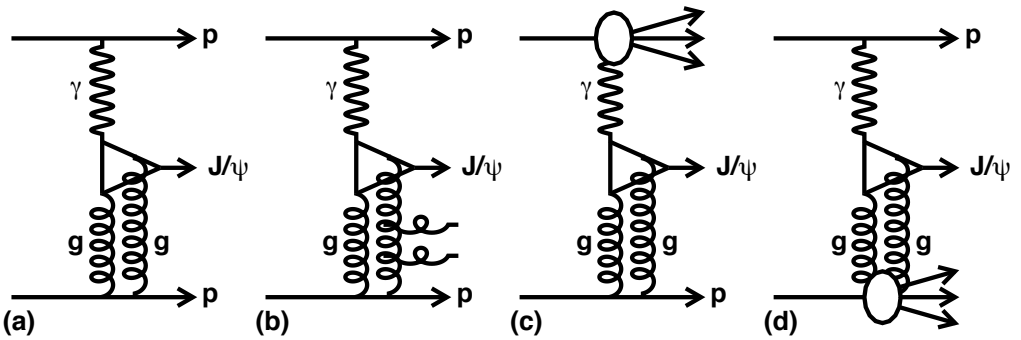

Figure 1: Feynman diagrams displaying (a) exclusive J/ψ and (b) inelastic J/ψ production where a small number of additional particles are produced due to gluon radiation and (c),(d) proton dissociation. Equivalent diagrams apply for $\psi(2S)$ production.

gluon PDF: $g(x, Q^2) \propto x^\lambda$ at the scale $Q^2 = M_{J/\psi}^2/4$, where $M_{J/\psi}$ is the mass of the J/ψ meson. All measurements to date at hadron machines are consistent with this, albeit with rather large uncertainties. However, higher-order corrections [5] or saturation effects [2, 3] lead to deviations from a pure power-law behaviour and the measurements presented here have sufficient precision to probe this effect. The $\psi(2S)$ differential cross-section measurements from the H1 collaboration are also consistent with a power-law function, although the limited data sample implies a rather large uncertainty and leads to a value for the exponent of $\delta = 0.91 \pm 0.17$ [13]. Both CDF and LHCb results are consistent with this.

This paper presents updated measurements from the LHCb collaboration using $930\,\text{pb}^{-1}$ of data collected in 2011 at $\sqrt{s} = 7$ TeV. Both the J/ψ and $\psi(2S)$ cross-sections are measured differentially as a function of meson rapidity and compared to various theoretical models, including those with saturation effects. The analysis technique is essentially that published previously [11]. The main difference concerns the methodology for determining the background due to non-exclusive J/ψ and $\psi(2S)$ production where the additional particles remain undetected.

2 Detector and data samples

The LHCb detector [14] is a single-arm forward spectrometer covering the pseudorapidity range $2 < \eta < 5$ (forward region), designed for the study of particles containing b or c quarks. The detector includes a high precision tracking system consisting of a silicon-strip vertex detector (VELO) surrounding the pp interaction region, a large-area silicon-strip detector (TT) located upstream of a dipole magnet with a bending power of about 4 Tm, and three stations of silicon-strip detectors (IT) and straw drift-tubes (OT) [15] placed downstream. The combined tracking system provides a momentum measurement with relative uncertainty that varies from 0.4% at $5\,\text{GeV}/c$ to 0.6% at $100\,\text{GeV}/c$, and impact parameter resolution of $20\,\mu\text{m}$ for tracks with large transverse momentum. Different types of charged hadrons are distinguished by information from two ring-imaging Cherenkov detectors [16]. Photon, electron and hadron candidates are identified by a calorimeter system consisting of scintillating-pad (SPD) and pre-shower detectors, an electromagnetic calorimeter and a hadronic calorimeter. The SPD also provides a measurement of the charged particle multiplicity in an event. Muons are identified by a system composed of alternating layers of iron and multiwire proportional chambers [17]. The trigger [18] consists of a hardware stage, based on information from the calorimeter and muon systems, followed by a software stage, which applies a full event reconstruction. The VELO also has sensitivity to charged particles with momenta above $\sim 100\,\text{MeV}/c$ in the pseudorapidity range $-3.5 < \eta < -1.5$ (backward region), while extending the sensitivity of the forward region to $1.5 < \eta < 5$.

The J/ψ and $\psi(2S)$ are identified through their decay to two muons. The protons are only marginally deflected by the peripheral collision and remain undetected inside the beam pipe. Therefore, the signature for exclusive vector meson production is an

event containing two muons and no other activity. Beam-crossings with multiple proton interactions produce additional activity; in the 2011 data-taking period the average number of visible interactions per bunch crossing was 1.4. Consequently, requiring an exclusive signature restricts the analysis to beam crossings with a single pp interaction.

The SuperChic [19] generator is used to produce samples of exclusive J/ψ and $\psi(2S)$ decays as well as those of the χ_c meson, which form a background for the J/ψ analysis. These are passed through a GEANT4 [20] based detector simulation, the trigger emulation and the event reconstruction chain of the LHCb experiment.

3 Event selection

The hardware trigger used in this analysis requires a single muon track with transverse momentum $p_{\rm T} > 400\,{\rm MeV}/c$ in coincidence with a low SPD multiplicity (< 10 hits). The software trigger used to select signal events requires two muons with $p_{\rm T} > 400$ MeV/c.

The analysis is performed in ten equally sized bins of meson rapidity between 2.0 and 4.5. The selection of exclusive events begins with the requirement of two reconstructed muons in the forward region. The acceptance of LHCb for muons from J/ψ and $\psi(2S)$ decays is not uniform: muons with low momenta can be swept out of the LHCb acceptance by the magnetic field, or be absorbed before they reach the muon stations. Consequently, a fiducial region is defined requiring that each muon has a momentum greater than 6 GeV/c and both tracks are reconstructed within the muon chamber acceptance. The fiducial acceptance is determined using simulated events and is shown in Fig. 2 for both J/ψ and $\psi(2S)$ decays, both of which are assumed to be transversely polarised due to s-channel helicity conservation. A systematic uncertainty of 2%, fully correlated between bins, is taken on these values corresponding to the estimated uncertainty on the description of the tracking in the simulation [21].

It is required that there are no photons reconstructed in the detector and no other tracks that incorporate VELO information. Unlike the previous analysis [11], a veto is not imposed on tracks constructed solely from TT and IT/OT detector combinations, as these

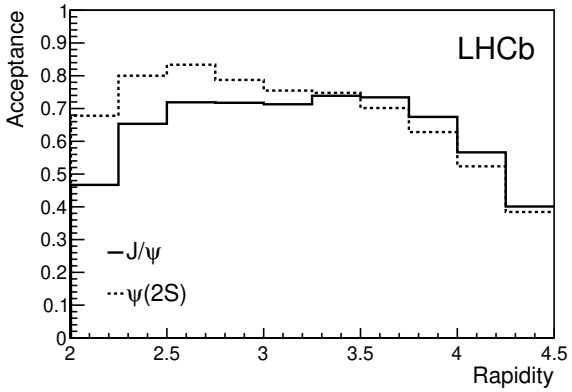

Figure 2: Acceptance for (solid) J/ψ and (dotted) $\psi(2S)$ decays as a function of their rapidity.

can arise from detector signals associated with previous beam interactions ("spillover"). The absence of activity apart from the two muons ensures two rapidity gaps which sum to 3.5 units in the forward region. An additional rapidity gap is obtained by requiring that there are no tracks in the backward region. The VELO is sensitive to tracks within a certain rapidity region depending on the z position from which the tracks originate and the event topology. The mean size of the backward rapidity gap that can be identified is 1.7 with a root mean square of about 0.5.

Muon pairs are combined to form meson candidates whose transverse momentum squared must satisfy $p_{\rm T}^2 < 0.8\,{\rm GeV}^2/c^2$, and whose invariant masses must lie within $65\,{\rm MeV}/c^2$ of the known J/ψ or $\psi(2S)$ mass values [22]. With these requirements, 55,985 J/ψ candidates and 1565 $\psi(2S)$ candidates are found.

Three background components are considered: non-resonant background due primarily to the QED process that produces two muons; feed-down from exclusive production of other mesons (*e.g.* χ_c); and inelastic production of mesons where one or both protons disassociate.

3.1 Non-resonant background determination

The invariant mass distributions for J/ψ and $\psi(2S)$ candidates are shown in Fig. 3 and are fitted with Crystal Ball functions [23] to describe the resonant contributions and an exponential function for the non-resonant background. Within the range of $\pm 65\,{\rm MeV}/c^2$ about the known meson masses, the non-resonant background is estimated to account for $(0.8 \pm 0.1)\%$ and $(17.0 \pm 0.3)\%$ of the J/ψ and $\psi(2S)$ candidates, respectively.

3.2 Feed-down background determination

Exclusively produced χ_c or $\psi(2S)$ mesons can feed down to mimic an exclusive J/ψ decay when the particles produced in association with the J/ψ remain undetected or go outside the detector acceptance. Their contribution is estimated using simulated events normalised to an enriched background sample in the data. Exclusive χ_c candidate events are identified in the data as those containing a J/ψ and a single photon [24]. The background from χ_c feed-down is then estimated by scaling the number of observed χ_c candidates by the ratio of simulated χ_c mesons passing the J/ψ selection requirements compared to those identified as χ_c candidate events. The feed-down from χ_c decays is estimated to account for $(7.6 \pm 0.9)\%$ of the exclusive J/ψ candidates, where the uncertainty includes a contribution from the fitted proportions of χ_{c0}, χ_{c1}, χ_{c2} as well as the photon reconstruction efficiency in simulation. Feed-down from $\psi(2S)$ decays is estimated by scaling the $\psi(2S)$ yields in the resonant peak (Fig. 3) by the ratio of simulated $\psi(2S)$ mesons passing the J/ψ selection requirements compared to those passing the $\psi(2S)$ selection requirements. The feed-down from $\psi(2S)$ decays is estimated to account for $(2.5 \pm 0.2)\%$ of the exclusive J/ψ candidates.

Feed-down into the $\psi(2S)$ selection is expected to be very small, *e.g.* due to $\chi_c(2P)$ or $X(3872)$ decays [25, 26]. Relaxing the requirement on the number of photons in the

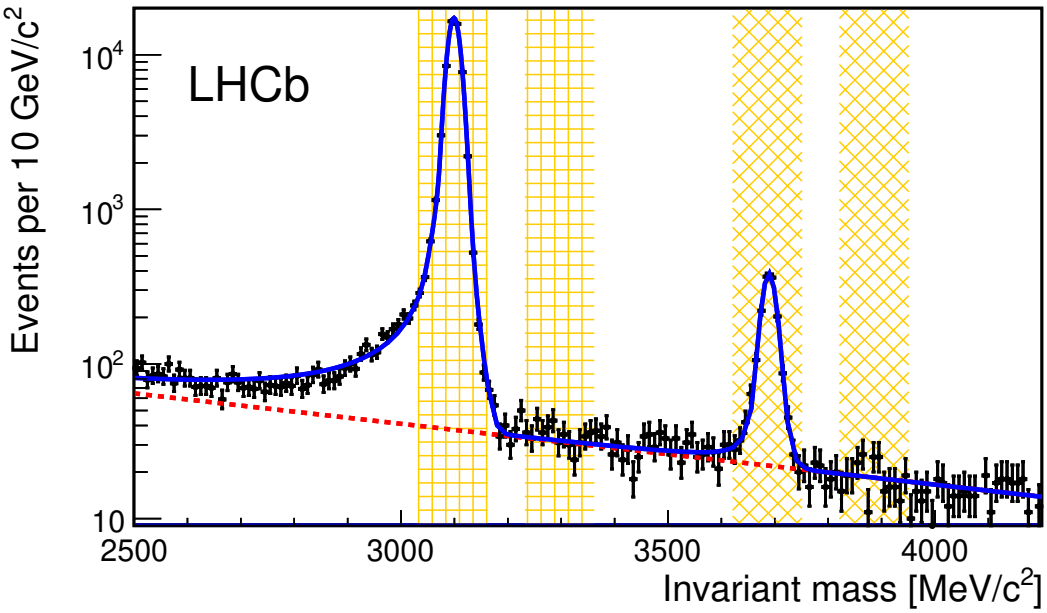

Figure 3: Invariant mass distribution of muon pairs after the selection requirements. The horizontally hatched regions show the J/ψ (left) signal and (right) side-band regions. The diagonally hatched regions show the $\psi(2S)$ (left) signal and (right) side-band regions. The data are fitted (solid curve) with Crystal Ball functions for the signals and an exponential function for the non-resonant background; the latter contribution is shown by the dashed curve.

selection, an additional 2% of $\psi(2S)$ candidates is selected, from which a feed-down of $(2.0 \pm 2.0)\%$ is estimated.

3.3 Inelastic background determination

The largest background is due to diffractive J/ψ and $\psi(2S)$ meson production with additional gluon radiation or proton dissociation (see Figs. 1(b),(c),(d)) where the particles produced go outside the LHCb acceptance and, in particular, close to the beam-line. Proton dissociation is more likely to occur when the transverse momentum of the meson is higher, while additional gluon radiation also increases the average $p_{\rm T}$. Thus the inelastic background has a higher $p_{\rm T}$ than the signal.

In Regge theory, it is assumed that for elastic J/ψ and $\psi(2S)$ meson production $d\sigma/dt \propto \exp(b_s t)$, where $t \approx -p_{\rm T}^2 c^2$ is the four-momentum transfer squared at the proton-pomeron vertex. The H1 and ZEUS collaborations confirmed this dependence and measured $b_{\rm s} = 4.88 \pm 0.15\,{\rm GeV}^{-2}$ [8] and $b_{\rm s} = 4.15 \pm 0.05^{+0.30}_{-0.18}\,{\rm GeV}^{-2}$ [9], respectively, for J/ψ production, while H1 measured $b_{\rm s} = 4.3 \pm 0.6\,{\rm GeV}^{-2}$ [13] for $\psi(2S)$ production. In contrast, the proton dissociative production of J/ψ or $\psi(2S)$ for $|t| < 1.2$ GeV^2 is observed to follow an exponential dependence, $\exp(b_{\rm pd} t)$, with $b_{\rm pd} = 1.07 \pm 0.11\,{\rm GeV}^{-2}$ for J/ψ and $b_{\rm pd} = 0.59 \pm 0.17\,{\rm GeV}^{-2}$ for $\psi(2S)$ [27]. For larger values of $|t|$ a power law is required [8].

The values of b measured at HERA can be extrapolated to LHC energies using Regge

theory: $b(W) = b_0 + 4\alpha' \log(W/W_0)$, with $W_0 = 90\,\text{GeV}$ and $\alpha' = 0.164 \pm 0.041\,\text{GeV}^{-2}$ [7] for the elastic process while $\alpha' = -0.014 \pm 0.009\,\text{GeV}^{-2}$ [27] for proton dissociation. This predicts $b_\text{s} \approx 6\,\text{GeV}^{-2}$ and $b_\text{pd} \approx 1\,\text{GeV}^{-2}$ in the LHCb kinematic region.

After the non-resonant contribution has been subtracted using the side-bands indicated in Fig. 3, and with the requirement of $p_\text{T}^2 < 0.8\,\text{GeV}^2/c^2$ for the J/ψ and $\psi(2S)$ removed, the data are fitted to the function

$$\frac{f_\text{s}}{N_1}\exp\left(-b_\text{s}p_\text{T}^2c^2\right) + \frac{f_\text{pd}}{N_2}\exp\left(-b_\text{pd}p_\text{T}^2c^2\right) + \frac{f_\text{fd}}{N_3}F_\text{fd}(p_\text{T}^2),$$

where f_s and f_pd are the fractions of elastic and proton-dissociative production, respectively, and f_fd is the fraction of feed-down fixed to that obtained in Sec. 3.2. The shape of the distribution for the feed-down contribution, F_fd, is taken from the data using $\chi_c \to J/\psi\,\gamma$ and $\psi(2S) \to J/\psi\,\pi\pi$ candidates. The numbers N_1, N_2 and N_3 normalise each of the three functions to unity in the region $p_\text{T}^2 < 0.8\,\text{GeV}^2/c^2$, while b_s and b_pd are free parameters.

The result of the fit for the J/ψ sample is shown in Fig. 4(a). The χ^2/ndf of the fit is 115/96 and returns values of $b_\text{s} = 5.70 \pm 0.11\,\text{GeV}^{-2}$ and $b_\text{pd} = 0.97 \pm 0.04\,\text{GeV}^{-2}$. Below $p_\text{T}^2 = 0.8\,\text{GeV}^2/c^2$, the signal fraction is 0.597 ± 0.012 and correcting for the non-resonant contribution gives an overall purity for the J/ψ sample of 0.592 ± 0.012. The result of the fit for the $\psi(2S)$ sample is shown in Fig. 4(b). The χ^2/ndf of the fit is 11/16 and returns values of $b_\text{s} = 5.1 \pm 0.7\,\text{GeV}^{-2}$ and $b_\text{pd} = 0.8 \pm 0.2\,\text{GeV}^{-2}$. Below $p_\text{T}^2 = 0.8\,\text{GeV}^2/c^2$, the signal fraction is 0.62 ± 0.08 and correcting for the non-resonant contribution gives an overall purity for the $\psi(2S)$ sample of 0.52 ± 0.07. In both cases, the values obtained for b_s and b_pd are in agreement with the extrapolations of HERA results using Regge theory.

A systematic uncertainty is assigned due to the choice of the fit range and the shape of the parameterisation describing the inelastic background. Doubling the range of the fit for the $\psi(2S)$ candidates changes the signal fraction by 3%. Doubling the range of the fit for the J/ψ candidates leads to a poor quality fit; a single exponential function does not describe the background well. For large values of p_T^2, the H1 collaboration introduced a function of the form $(1 + b_\text{pd}p_\text{T}^2/n)^{-n}$ which interpolates between an exponential at low

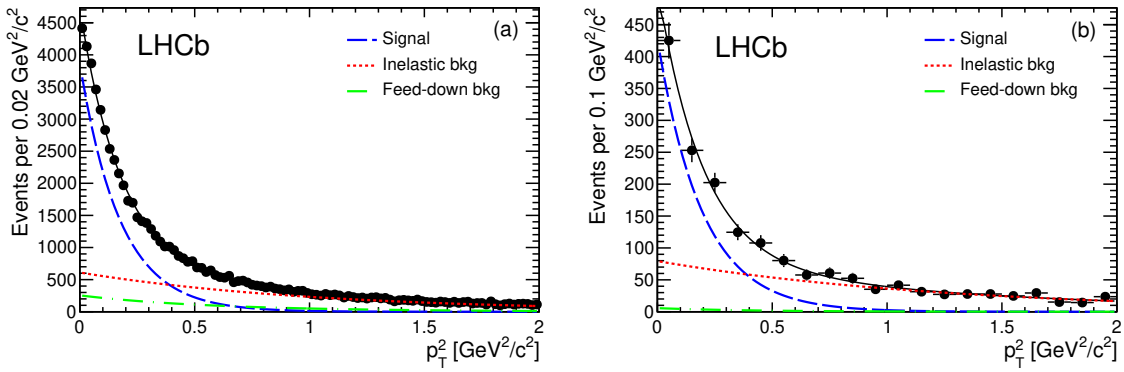

Figure 4: Transverse momentum squared distributions for (a) J/ψ and (b) $\psi(2S)$ candidates, where the non-resonant background contribution has been subtracted using side-bands. The points are data, the solid curve is the total fit while the different contributions are as described.

$p_{\rm T}^2$ and a power law at high $p_{\rm T}^2$ [8]. Using this functional form and holding $n = 3.58$, as determined by H1, gives an acceptable fit with the signal fraction changing by 5%. This value is used as a systematic uncertainty on the purity determination for both the J/ψ and $\psi(2S)$ analyses.

The calculated fraction of feed-down is found to have a negligible effect on the fraction of signal events as the shapes are similar to the fitted shape for the proton dissociation. The purity of the sample is also calculated in bins of rapidity. No trends are observed and all values are consistent within statistical uncertainties. Consequently a single value for the purity of each sample is assumed, independent of the rapidity of the meson.

4 Cross-section calculation

The cross-section times branching fraction to two muons with pseudorapidities between 2.0 and 4.5 is calculated in ten bins of meson rapidity, y, via

$$\left(\frac{d\sigma}{dy}\right)_i = \frac{\rho N_i}{A_i \epsilon_i \Delta y (\epsilon_{\rm single} L)}, \tag{1}$$

where: N_i is the number of events in bin i; ρ is the purity of the sample as described in the previous section; A_i is the acceptance of the fiducial region as shown in Fig. 2; ϵ_i is the efficiency to select a signal event; Δy is the bin width; L is the luminosity, which has been determined with an uncertainty of 3.5% [28]; and $\epsilon_{\rm single}$ is the efficiency for selecting single interaction events, which accounts for the fact that the selection requirements reject signal events that are accompanied by a visible proton-proton interaction in the same beam crossing.

The number of visible proton-proton interactions per beam crossing, n, is assumed to follow a Poisson distribution, $P(n) = \mu^n \exp(-\mu)/n!$, where μ is the average number of visible interactions, defined as interactions with one or more tracks having VELO information. The probability that a signal event is not rejected due to the presence of another visible interaction is given by $P(0)$ and therefore, $\epsilon_{\rm single} = \exp(-\mu)$. This has been calculated throughout the data-taking period in roughly hour-long intervals; variations in μ during this interval have been studied and found to have a negligible effect. The spread in the value of μ for different crossing bunch-pairs is small and its effect is neglected. Spillover from previous beam crossings does not affect the VELO, and detector noise is typically at the level of a few uncorrelated hits, which do not form a track. Averaged over the data-taking period, $\epsilon_{\rm single} = 0.241 \pm 0.003$, where the uncertainty has been calculated with the assumption that at least one track in a visible interaction may be spurious.

For events with two tracks inside the fiducial region, the efficiency to select a meson can be expressed as the product $\epsilon_{\rm id}^{\psi} \times \epsilon_{\rm trig}^{\psi} \times \epsilon_{\rm sel}$, where $\epsilon_{\rm id}^{\psi}$ is the efficiency for both tracks from the meson to be identified as muons, $\epsilon_{\rm trig}^{\psi}$ is the efficiency for an event with two reconstructed muons to fire the triggers, and $\epsilon_{\rm sel}$ is the efficiency for a triggered event to pass the selection criteria. Most of these quantities are calculated directly from the data.

For muons coming from J/ψ decays, a tag-and-probe technique is used to find the efficiency to identify a single muon, $\epsilon^{\mu}_{\rm id}(\phi,\eta)$, as a function of the azimuthal angle, ϕ, and pseudorapidity, η. The tag is an identified muon that fires the trigger. The probe is the other track in events with precisely two tracks, which gives the J/ψ invariant mass when combined with the tag-track. The fraction of probes identified as muons determines $\epsilon^{\mu}_{\rm id}(\phi,\eta)$ from which $\epsilon^{\psi}_{\rm id}(y)$ is found using the simulation to relate the rapidity of the meson to the azimuthal angles and pseudorapidities of the two muons. A scaling factor (typically 1%), found using simulated events, is applied to get the corresponding quantity for muons from $\psi(2S)$ decays, which have a slightly different momentum spectrum due to the higher mass of the $\psi(2S)$ meson.

In a similar way, the tag-and-probe technique is used to find the efficiency for a single muon to fire the hardware trigger, from which is derived the corresponding J/ψ efficiency. The software trigger requires the presence of two muons. Its efficiency is determined using an independent pre-scaled software trigger that fires on a single muon. Combining these factors together gives a data-driven estimate of $\epsilon^{\psi}_{\rm trig}$ for J/ψ decays. A correction of typically 3%, found using simulated events, is applied to get the corresponding quantity for $\psi(2S)$ decays. The values determined for $\epsilon^{\psi}_{\rm id}\times\epsilon^{\psi}_{\rm trig}$ as a function of rapidity are given in Table 1.

The selection efficiency, $\epsilon_{\rm sel}$, is determined using simulation and data. From simulation the requirement of having no additional tracks in the event has an efficiency of 0.997 ± 0.001, and the requirement that $p_{\rm T}^2 < 0.8$ GeV$^2/c^2$ has an efficiency of 0.979 ± 0.003, where the uncertainty corresponds to a change of 5% in the value of $b_{\rm s}$ used in the simulation. The simulation, calibrated using a sample of $J/\psi+\gamma$ candidates in data, determines the efficiency for having no identified photons in the event to be 0.972 ± 0.005. The requirement that the meson mass lies within 65 MeV of the known value is found from the fit in Fig. 3 and gives an efficiency of 0.96 ± 0.01. The global requirement, imposed by the hardware trigger, that there be fewer than ten SPD hits introduces a small inefficiency due to spillover from previous beam crossings. The efficiency of the SPD requirement is measured to be 0.96 ± 0.01 using an independent trigger that has no constraint on the number of SPD hits. Combining these together, it is estimated that $\epsilon_{\rm sel}=0.87\pm0.01$ for the J/ψ selection and the same value is taken for the $\psi(2S)$ analysis.

The numbers entering the cross-section calculation are summarised in Table 1. Applying Eq. 1 leads to differential cross-section times branching fraction values for mesons with both muons inside $2.0<\eta_{\mu^\pm}<4.5$, which are reported in Table 2. The uncorrelated statistical uncertainties are combined in quadrature and are reported in the top half of the table. The statistical uncertainties on $\epsilon_{\rm sel}$ and the purity are correlated between bins and are quoted in the lower half of the table. The systematic uncertainties on the fraction of single interaction beam-crossings, the acceptance, the shape of the inelastic background and the luminosity are also correlated between bins and are indicated separately.

The total cross-section times branching fraction to two muons is obtained by integrating the cross-sections in Table 2. The uncorrelated statistical uncertainties are added in quadrature and combined with the correlated ones to give the total statistical uncertainty. The correlated systematic uncertainties, indicated in the lower part of Table 2 by asterisks,

Table 1: Quantities entering the cross-section calculations as a function of meson rapidity.

y range (J/ψ)	$[2.00, 2.25]$	[2.25,2.50]	[2.50,2.75]	[2.75,3.00]	[3.00,3.25]
# Events	798	3911	6632	8600	9987
Acceptance	0.467 ± 0.009	0.653 ± 0.013	0.719 ± 0.014	0.718 ± 0.014	0.713 ± 0.014
$\epsilon^{\psi}_{\rm id} \times \epsilon^{\psi}_{\rm trig}$	0.71 ± 0.03	0.78 ± 0.02	0.81 ± 0.01	0.84 ± 0.01	0.85 ± 0.01
Purity	$0.592 \pm 0.012 \pm 0.030$				

y range (J/ψ)	$[3.25, 3.50]$	[3.50,3.75]	[3.75,4.00]	[4.00,4.25]	[4.25,4.50]
# Events	9877	7907	5181	2496	596
Acceptance	0.739 ± 0.015	0.734 ± 0.015	0.674 ± 0.014	0.566 ± 0.011	0.401 ± 0.008
$\epsilon^{\psi}_{\rm id} \times \epsilon^{\psi}_{\rm trig}$	0.87 ± 0.01	0.88 ± 0.01	0.87 ± 0.01	0.83 ± 0.02	0.81 ± 0.03
Purity	$0.592 \pm 0.012 \pm 0.030$				

y range ($\psi(2S)$)	$[2.00, 2.25]$	[2.25,2.50]	[2.50,2.75]	[2.75,3.00]	[3.00,3.25]
# Events	31	111	208	1287	268
Acceptance	0.678 ± 0.013	0.800 ± 0.016	0.834 ± 0.017	0.787 ± 0.016	0.755 ± 0.015
$\epsilon^{\psi}_{\rm id} \times \epsilon^{\psi}_{\rm trig}$	0.80 ± 0.03	0.83 ± 0.02	0.86 ± 0.01	0.88 ± 0.01	0.88 ± 0.01
Purity ($\psi(2S)$)	$0.52 \pm 0.07 \pm 0.03$				

y range($\psi(2S)$)	$[3.25, 3.50]$	[3.50,3.75]	[3.75,4.00]	[4.00,4.25]	[4.25,4.50]
# Events	282	201	105	61	11
Acceptance	0.748 ± 0.015	0.702 ± 0.014	0.628 ± 0.013	0.524 ± 0.010	0.384 ± 0.008
$\epsilon^{\psi}_{\rm id} \times \epsilon^{\psi}_{\rm trig}$	0.90 ± 0.01	0.89 ± 0.01	0.87 ± 0.01	0.84 ± 0.02	0.77 ± 0.03
Purity ($\psi(2S)$)	$0.52 \pm 0.07 \pm 0.03$				

y range (J/ψ and $\psi(2S)$)	$[2.00, 4.50]$
$\epsilon_{\rm sel}$	0.87 ± 0.01
$\epsilon_{\rm single}$	0.241 ± 0.003
L ($\rm pb^{-1}$)	929 ± 33

are combined to give the total systematic uncertainty. This leads to the following results for the cross-section times branching fraction to two muons having pseudorapidities between 2.0 and 4.5:

$$\begin{aligned} \sigma_{pp\to J/\psi\to\mu^+\mu^-}(2.0 < \eta_{\mu^\pm} < 4.5) = &\quad 291 \pm 7 \pm 19\,\text{pb}, \\ \sigma_{pp\to\psi(2S)\to\mu^+\mu^-}(2.0 < \eta_{\mu^\pm} < 4.5) = &\quad 6.5 \pm 0.9 \pm 0.4\,\text{pb}, \end{aligned} \tag{2}$$

where the first uncertainty is statistical and the second is systematic.

The differential cross-section results reported in Table 2 correspond to muons that enter the LHCb detector fiducial volume. Differential cross-section results as a function of meson rapidity are obtained by dividing by the known meson branching fraction to two muons [22] and by the fraction of decays with $2.0 < \eta_{\mu^\pm} < 4.5$. The former introduces an

Table 2: Differential cross-section times branching ratio, in units of pb, for mesons decaying to two muons, both with $2.0 < \eta < 4.5$, in bins of meson rapidity. Only the uncorrelated statistical uncertainties are quoted with the central values. The uncertainties, correlated between bins, are tabulated in the lower table. Those with an asterisk enter into the systematic uncertainty.

y range	$[2.00, 2.25]$	[2.25,2.50]	[2.50,2.75]	[2.75,3.00]	[3.00,3.25]
$\frac{d\sigma}{dy}$ J/ψ	29.3 ± 1.7	92.5 ± 2.4	137.8 ± 2.4	173.1 ± 2.6	198.0 ± 2.7
$\frac{d\sigma}{dy}$ $\psi(2S)$	0.56 ± 0.11	1.75 ± 0.17	3.06 ± 0.22	4.41 ± 0.26	4.24 ± 0.26

y range	$[3.25, 3.50]$	[3.50,3.75]	[3.75,4.00]	[4.00,4.25]	[4.25,4.50]
$\frac{d\sigma}{dy}$ J/ψ	187.6 ± 2.6	148.9 ± 2.4	107.4 ± 2.1	65.3 ± 2.0	21.9 ± 1.3
$\frac{d\sigma}{dy}$ $\psi(2S)$	4.51 ± 0.27	3.43 ± 0.25	2.05 ± 0.20	1.47 ± 0.19	0.36 ± 0.11

Correlated uncertainties expressed as a percentage of the final result	
ϵ_{sel}	1.4%
Purity determination (J/ψ)	2.0%
Purity determination ($\psi(2S)$)	13.0%
$^*\epsilon_{\text{single}}$	1.0%
*Acceptance	2.0%
*Shape of the inelastic background	5.0%
*Luminosity	3.5%
Total correlated statistical uncertainty (J/ψ)	2.4%
Total correlated statistical uncertainty ($\psi(2S)$)	13.0%
Total correlated systematic uncertainty	6.5%

Table 3: Fraction of events in a given meson rapidity range where both muons have $2.0 < \eta < 4.5$.

y range	$[2.00, 2.25]$	[2.25,2.50]	[2.50,2.75]	[2.75,3.00]	[3.00,3.25]
Acceptance	0.093	0.289	0.455	0.617	0.735

y range	$[3.25, 3.50]$	[3.50,3.75]	[3.75,4.00]	[4.00,4.25]	[4.25,4.50]
Acceptance	0.738	0.624	0.470	0.286	0.103

additional systematic uncertainty of 10% for the $\psi(2S)$ measurement. The latter depends on the kinematics of the decay, is calculated using SuperChic assuming that the J/ψ and $\psi(2S)$ mesons are transversely polarised, and is given in Table 3.

Table 4: Comparison of this result to various theoretical predictions.

	J/ψ [pb]	$\psi(2S)$ [pb]
Gonçalves and Machado [29]	275	
JMRT [5]	282	8.3
Motyka and Watt [2]	334	
Schäfer and Szczurek [30]	317	
Starlight [31]	292	6.1
SUPERCHIC [19]	317	7.0
LHCb measured value	$291 \pm 7 \pm 19$	$6.5 \pm 0.9 \pm 0.4$

5 Discussion

The integrated cross-section measurements for J/ψ and $\psi(2S)$ mesons decaying to muons with $2.0 < \eta_{\mu^\pm} < 4.5$ are compared to various theoretical predictions in Table 4. Good agreement is found in each case.

The differential distribution for J/ψ production is presented in Fig. 5(a), where the extent of the error bars indicates the uncorrelated statistical uncertainties and the band is the total uncertainty. Jones, Martin, Ryskin and Teubner (JMRT) [5] have obtained leading-order (LO) and next-to-leading-order [1] (NLO) predictions from a fit to HERA and LHCb 2010 data, which are dominated by the HERA data; thus these curves can be considered as LO and NLO extrapolations from HERA energies. The LO result is essentially the power-law photoproduction result from HERA, combined with a photon flux function and a gap survival factor [32]. Better agreement is obtained between data and the NLO prediction than between data and the LO prediction.

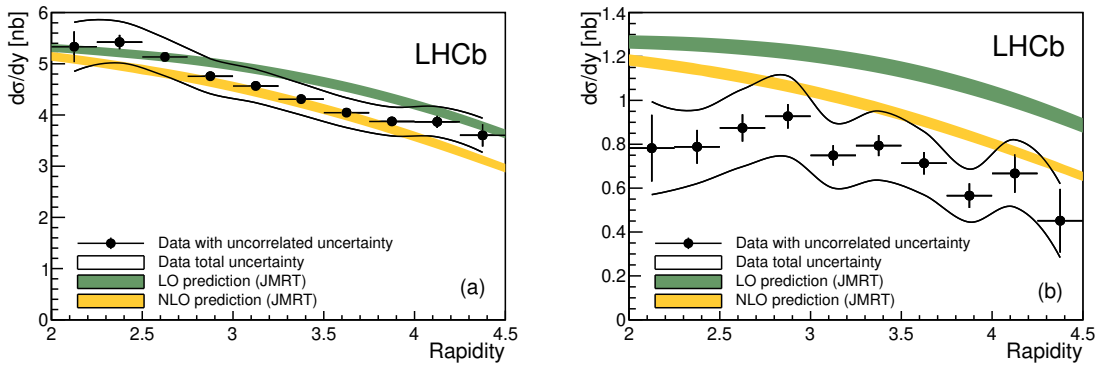

Figure 5: Differential cross-section for (a) J/ψ and (b) $\psi(2S)$ production compared to LO and NLO predictions of [5]. The band indicates the total uncertainty, most of which is correlated between bins.

[1] Only the dominant NLO corrections have been considered: see [5] for details.

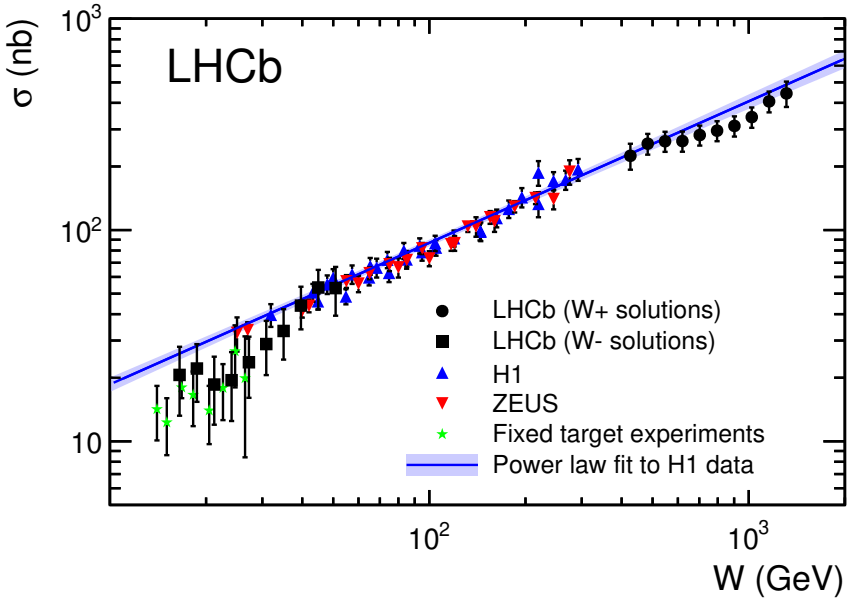

Figure 6: Photoproduction cross-section as a function of the centre-of-mass of the photon-proton system with the power-law fit from [8] superimposed. The LHCb data points for $W_+(W_-)$ are derived assuming the power-law fit for $W_-(W_+)$. The uncertainties are correlated between bins. Fixed target results are from the E401 [33], E516 [34] and E687 [35] collaborations.

Exclusive production of J/ψ in pp collisions is related to photoproduction through

$$\frac{d\sigma}{dy}_{pp\to pJ/\psi p} = r_+ k_+ \frac{dn}{dk_+}\sigma_{\gamma p\to J/\psi p}(W_+) + r_- k_- \frac{dn}{dk_-}\sigma_{\gamma p\to J/\psi p}(W_-) \qquad (3)$$

where $dn/dk_\pm$ are photon fluxes for photons of energy $k_\pm \approx (M_{J/\psi}/2)\exp(\pm|y|)$, $(W_\pm)^2 = 2k_\pm\sqrt{s}$, and $r_\pm$ are absorptive corrections as given, for example, in [5, 30]. The LHCb results cannot unambiguously determine the photoproduction cross-section due to contributions from both W_+ and W_-, corresponding to the photon being either an emitter or a target, respectively. However, a comparison can be made to the HERA photoproduction results using the power-law relationship, $\sigma_{\gamma p\to J/\psi p}(W) = 81(W/90\,\text{GeV})^{0.67}$ nb, determined by the H1 collaboration [8]. A model-dependent measurement of $\sigma_{\gamma p\to J/\psi p}(W_+)$ is obtained from the LHCb differential cross-section measurement by applying Eq. 3 and assuming the power-law result for $\sigma_{\gamma p\to J/\psi p}(W_-)$, while $\sigma_{\gamma p\to J/\psi p}(W_-)$ is obtained by assuming the power-law result for $\sigma_{\gamma p\to J/\psi p}(W_+)$. The result of this procedure is shown in Fig. 6, which compares the modified LHCb data with HERA and fixed target photoproduction results: note that there are two correlated points plotted for each LHCb measurement, corresponding to the W_+ and W_- solutions. It was shown in our previous publication [11] that the LHCb data were consistent, within large statistical uncertainties, with a simple power-law extrapolation of HERA J/ψ photoproduction results to LHC energies. With increased statistics, an extrapolation of the power-law obtained in [8] is in marginal agreement with the LHCb data.

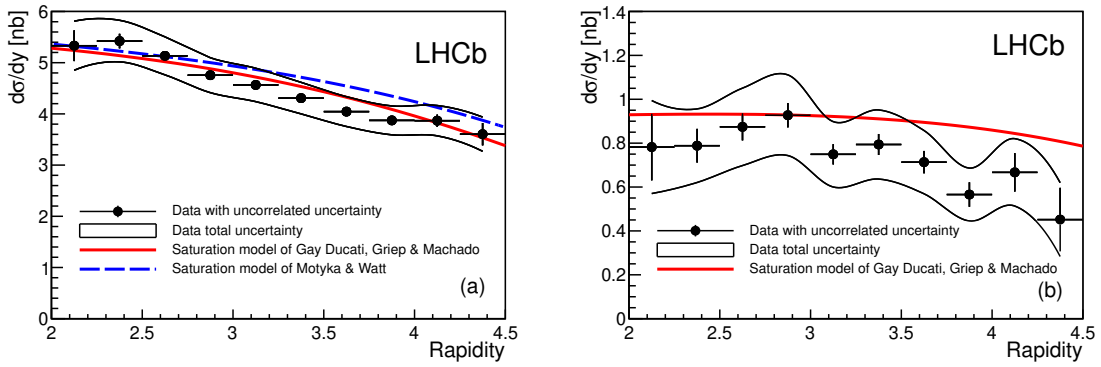

Figure 7: Differential distribution for (a) J/ψ and (b) $\psi(2S)$ compared to the predictions of Gay Ducati, Griep and Machado [3] and Motyka and Watt [2], which include saturation effects. The points are data where the error bars indicate the uncorrelated uncertainties. The band indicates the total uncertainty, most of which is correlated between bins.

The differential distribution for $\psi(2S)$ production is presented in Fig. 5(b) and is compared to both LO and NLO predictions [2] from JMRT [36] using the formalism described in [5] with the gluon PDF taken from their J/ψ analysis. Once again, better agreement is found between data and the NLO prediction than between data and the LO prediction.

In addition to higher order effects being capable of explaining the deviation from a pure power-law behaviour, saturation effects may be important. Figure 7(a) compares the J/ψ differential distribution to predictions by Motyka and Watt [2] and Gay Ducati, Griep and Machado [3], that both include saturation effects and have a precision of $10-15\%$. A rapidity gap survival factor of $r(y) = 0.85 - 0.1|y|/3$ has been applied to the former while the latter assumes $r(y) = 0.8$. Both predictions use a Weizsäcker-Williams approximation to describe the photon flux. The agreement with the LHCb data is good. Figure 7(b) compares the $\psi(2S)$ differential distribution to the prediction of Gay Ducati, Griep and Machado. Good agreement with the data is again observed.

6 Conclusions

The differential and integrated cross-section times branching fraction for J/ψ and $\psi(2S)$ mesons decaying to two muons, both with $2.0 < \eta < 4.5$, have been measured. The results of this analysis are consistent with the previously published LHCb analysis, which used data taken in 2010, but have a significantly improved precision, as well as a more extensive use of data-driven techniques to estimate systematic sources. An increase in luminosity, lower pile-up running conditions, as well as improvements in the trigger lead to roughly 40 times as many events in the 2011 data-taking period. The integrated cross-section

[2] These predictions were made by replacing the J/ψ mass and electronic width by those of the $\psi(2S)$ neglecting possible relativistic corrections, which may be important for the heavier meson.

measurements have an overall uncertainty that is a factor two better; they are limited by the theoretical modelling of the inelastic background for the J/ψ analysis and by the statistical precision with which the background is determined for the $\psi(2S)$ analysis. The cross-section is presented differentially for the $\psi(2S)$ for the first time. Although the total uncertainty for the J/ψ differential distribution is 7% per rapidity bin, most of this is correlated bin-to-bin; the uncorrelated uncertainty is typically 1.5%. Thus the overall shape of the differential distribution is rather well determined and this improves the ability of the data to distinguish between different theoretical models.

The integrated cross-sections are in good agreement with several theoretical estimates. The differential J/ψ and $\psi(2S)$ cross-section both agree better with the NLO rather than LO predictions of [5]. The result has also been compared to two models that include saturation effects [2, 3]; in both cases, good agreement is observed. It is also worth noting that the t-dependence for LHCb and HERA results are in agreement with Regge theory.

Acknowledgements

We thank Lucian Harland-Lang and Stephen Jones for many helpful discussions and clarifications. We express our gratitude to our colleagues in the CERN accelerator departments for the excellent performance of the LHC. We thank the technical and administrative staff at the LHCb institutes. We acknowledge support from CERN and from the national agencies: CAPES, CNPq, FAPERJ and FINEP (Brazil); NSFC (China); CNRS/IN2P3 and Region Auvergne (France); BMBF, DFG, HGF and MPG (Germany); SFI (Ireland); INFN (Italy); FOM and NWO (The Netherlands); SCSR (Poland); MEN/IFA (Romania); MinES, Rosatom, RFBR and NRC "Kurchatov Institute" (Russia); MinECo, XuntaGal and GENCAT (Spain); SNSF and SER (Switzerland); NAS Ukraine (Ukraine); STFC (United Kingdom); NSF (USA). We also acknowledge the support received from the ERC under FP7. The Tier1 computing centres are supported by IN2P3 (France), KIT and BMBF (Germany), INFN (Italy), NWO and SURF (The Netherlands), PIC (Spain), GridPP (United Kingdom). We are thankful for the computing resources put at our disposal by Yandex LLC (Russia), as well as to the communities behind the multiple open source software packages that we depend on.

References

[1] M. G. Ryskin, *Diffractive J/ψ electroproduction in LLA QCD*, Z. Phys. **C57** (1993) 89.

[2] L. Motyka and G. Watt, *Exclusive photoproduction at the Fermilab Tevatron and CERN LHC within the dipole picture*, Phys. Rev. **D78** (2008) 014023, arXiv:0805.2113.

[3] M. B. Gay Ducati, M. T. Griep, and M. V. T. Machado, *Exclusive photoproduction of J/ψ and $\psi(2S)$ states in proton-proton collisions at the CERN LHC*, arXiv:1305.4611.

[4] A. D. Martin, C. Nockles, M. G. Ryskin, and T. Teubner, *Small x gluon from exclusive J/ψ production*, Phys. Lett. **B662** (2008) 252, arXiv:0709.4406.

[5] S. Jones, A. Martin, M. Ryskin, and T. Teubner, *Probes of the small x gluon via exclusive J/ψ and Υ production at HERA and the LHC*, JHEP **1311** (2013) 085, arXiv:1307.7099.

[6] A. Bzdak, L. Motyka, L. Szymanowski, and J.-R. Cudell, *Exclusive J/ψ and Υ hadroproduction and the QCD odderon*, Phys. Rev. **D75** (2007) 094023, arXiv:hep-ph/0702134.

[7] H1 collaboration, A. Aktas *et al.*, *Elastic J/ψ production at HERA*, Eur. Phys. J. **C46** (2006) 585, arXiv:hep-ex/0510016.

[8] H1 collaboration, C. Alexa *et al.*, *Elastic and proton-dissociative photoproduction of J/ψ mesons at HERA*, Eur. Phys. J. **C73** (2013) 2466, arXiv:1304.5162.

[9] ZEUS collaboration, S. Chekanov *et al.*, *Exclusive photoproduction of J/ψ mesons at HERA*, Eur. Phys. J. **C24** (2002) 345, arXiv:hep-ex/0201043.

[10] CDF collaboration, T. Aaltonen *et al.*, *Observation of exclusive charmonium production and $\gamma\gamma \to \mu^+\mu^-$ in $p\bar{p}$ collisions at $\sqrt{s} = 1.96$ TeV*, Phys. Rev. Lett. **102** (2009) 242001, arXiv:0902.1271.

[11] LHCb collaboration, R. Aaij *et al.*, *Exclusive J/ψ and $\psi(2S)$ production in pp collisions at $\sqrt{s} = 7$ TeV*, J. Phys. **G40** (2013) 045001, arXiv:1301.7084.

[12] ALICE collaboration, B. Abelev *et al.*, *Coherent J/ψ photoproduction in ultra-peripheral Pb-Pb collisions at $\sqrt{s_{NN}} = 2.76$ TeV*, Phys. Lett. **B718** (2013) 1273, arXiv:1209.3715.

[13] H1 collaboration, C. Adloff *et al.*, *Diffractive photoproduction of $\psi(2S)$ mesons at HERA*, Phys. Lett. **B541** (2002) 251, arXiv:hep-ex/0205107.

[14] LHCb collaboration, A. A. Alves Jr. *et al.*, *The LHCb detector at the LHC*, JINST **3** (2008) S08005.

[15] R. Arink *et al.*, *Performance of the LHCb Outer Tracker*, arXiv:1311.3893.

[16] M. Adinolfi *et al.*, *Performance of the LHCb RICH detector at the LHC*, Eur. Phys. J. **C73** (2013) 2431, arXiv:1211.6759.

[17] A. A. Alves Jr. *et al.*, *Performance of the LHCb muon system*, JINST **8** (2013) P02022, arXiv:1211.1346.

[18] R. Aaij *et al.*, *The LHCb Trigger and its Performance in 2011*, JINST **8** (2013) P04022, arXiv:1211.3055.

[19] L. A. Harland-Lang, V. A. Khoze, M. G. Ryskin, and W. J. Stirling, *Central exclusive χ_c meson production at the Tevatron revisited*, Eur. Phys. J. **C65** (2010) 433, arXiv:0909.4748.

[20] GEANT4, S. Agostinelli *et al.*, *GEANT4: a simulation toolkit*, Nucl. Instrum. Meth. **A506** (2003) 250.

[21] A. Jaeger *et al.*, *Measurement of the track finding efficiency*, CERN-LHCb-PUB-2011-025.

[22] Particle Data Group, K. Nakamura *et al.*, *Review of particle physics*, J. Phys. **G37** (2010) 075021.

[23] T. Skwarnicki, *A study of the radiative cascade transitions between the Upsilon-prime and Upsilon resonances*, PhD thesis, Institute of Nuclear Physics, Krakow, 1986, DESY-F31-86-02.

[24] LHCb collaboration, *Central Exclusive Dimuon Production at $\sqrt{s} = 7$ TeV*, CERN-LHCb-CONF-2011-022.

[25] BaBar collaboration, B. Aubert *et al.*, *Evidence for $X(3872) \to \psi_{2S}\gamma$ in $B^{\pm} \to X(3872)K^{\pm}$ decays, and a study of $B \to c\bar{c}\gamma K$*, Phys. Rev. Lett. **102** (2009) 132001, arXiv:0809.0042.

[26] Belle collaboration, V. Bhardwaj *et al.*, *Observation of $X(3872) \to J/\psi\gamma$ and search for $X(3872) \to \psi'\gamma$ in B decays*, Phys. Rev. Lett. **107** (2011) 091803, arXiv:1105.0177.

[27] H1 collaboration, A. Aktas *et al.*, *Diffractive photoproduction of J/ψ mesons with large momentum transfer at HERA*, Phys. Lett. **B568** (2003) 205, arXiv:hep-ex/0306013.

[28] LHCb collaboration, R. Aaij *et al.*, *Absolute luminosity measurements with the LHCb detector at the LHC*, JINST **7** (2012) P01010, arXiv:1110.2866.

[29] V. P. Gonçalves and M. V. T. Machado, *Vector meson production in coherent hadronic interactions: an update on predictions for RHIC and LHC*, Phys. Rev. **C84** (2011) 011902, arXiv:1106.3036.

[30] W. Schäfer and A. Szczurek, *Exclusive photoproduction of J/ψ in proton-proton and proton-antiproton scattering*, Phys. Rev. **D76** (2007) 094014, arXiv:0705.2887.

[31] S. R. Klein and J. Nystrand, *Photoproduction of quarkonium in proton proton and nucleus nucleus collisions*, Phys. Rev. Lett. **92** (2004) 142003, arXiv:hep-ph/0311164.

[32] V. A. Khoze, A. D. Martin, and M. G. Ryskin, *Diffraction at the LHC*, Eur. Phys. J. **C73** (2013) 2503, arXiv:1306.2149.

[33] M. E. Binkley *et al.*, *J/ψ photoproduction from 60-GeV/c to 300-GeV/c*, Phys. Rev. Lett. **48** (1982) 73.

[34] B. H. Denby *et al.*, *Inelastic and elastic photoproduction of J/ψ (3097)*, Phys. Rev. Lett. **52** (1984) 795.

[35] E687 collaboration, P. L. Frabetti *et al.*, *A measurement of elastic J/ψ photoproduction cross-section at Fermilab E687*, Phys. Lett. **B316** (1993) 197.

[36] S. P. Jones, A. D. Martin, M. G. Ryskin, and T. Teubner, *Predictions of exclusive $\psi(2S)$ production at the LHC*, arXiv:1312.6795.